BOLETIN DE LA SOCIEDAD ESPAÑOLA DE
Cerámica y Vidrio
www.elsevier.es/bsecv

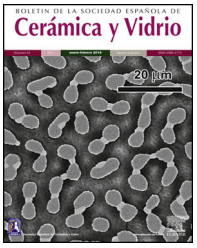

Microwave-assisted hydrothermal synthesis of nanocrystalline zirconia

Juan Carlos Fariñas

Instituto de Cerámica y Vidrio (ICV), CSIC, Madrid, Spain

ARTICLE INFO

Article history:
Received 21 March 2025
Accepted 24 April 2025
Available online 5 June 2025

Keywords:
Microwave-assisted hydrothermal synthesis
Quantitative precipitation
Nanocrystal
Zirconia
Monoclinic and tetragonal phases

ABSTRACT

A simple, fast and energy efficient microwave-assisted hydrothermal method was developed for the preparation of nanocrystalline zirconia from commercially available $ZrOCl_2 \cdot 8H_2O$ and KOH. The synthesis was conducted at 180 °C for 20 min by two ways: direct decomposition of $ZrOCl_2 \cdot 8H_2O$ (sample Z), and precipitation of $ZrOCl_2 \cdot 8H_2O$ with KOH and dehydration of hydroxides (sample ZK). The as-synthesized powders were calcined at 500 °C, and all the resulting products were characterized by XRD, FE-SEM, HR-TEM and SAED. Both the as-synthesized and calcined nanoparticles were highly crystalline. A single monoclinic phase was obtained for sample Z, while for sample ZK a tetragonal phase was achieved as the main phase with a minor fraction of monoclinic. The particles of the as-synthesized sample Z showed irregular and semi-hexagonal shapes, although they changed to spherical or ellipsoidal shapes during heat treatment. The particles of the sample ZK, both as-synthesized and calcined, exhibited nearly spherical or ellipsoidal shapes. The average crystallite size for the as-synthesized samples Z and ZK were 3.2 ± 0.8 and 5.5 ± 0.9 nm, respectively, while for the calcined ones the values were 8.5 ± 1.2 and 7.6 ± 1.2 nm, respectively.

Síntesis hidrotermal asistida por microondas de circona nanocristalina

Palabras clave:
Síntesis hidrotermal asistida por microondas
Precipitación cuantitativa
Nanocristal
Circona
Fases monoclínica y tetragonal

RESUMEN

Se ha desarrollado un método hidrotermal asistido por microondas, simple, rápido y eficiente energéticamente, para la preparación de circona nanocristalina a partir de $ZrOCl_2 \cdot 8H_2O$ y KOH comercialmente disponibles. La síntesis se ha realizado a 180 °C durante 20 min por dos caminos: descomposición directa de $ZrOCl_2 \cdot 8H_2O$ (muestra Z), y precipitación de $ZrOCl_2 \cdot 8H_2O$ con KOH y deshidratación de hidróxidos (muestra ZK). Los polvos sintetizados fueron calcinados a 500 °C, y todos los productos resultantes fueron caracterizados por *XRD*, *FE-SEM*, *HR-TEM* y *SAED*. Tanto las nanopartículas sintetizadas como las calcinadas

E-mail address: jcfarinas@icv.csic.es
https://doi.org/10.1016/j.bsecv.2025.100445

fueron altamente cristalinas. En el caso de la muestra Z, se obtuvo únicamente fase monoclínica, mientras que, en el caso de la muestra ZK, se obtuvo fase tetragonal como fase principal con una pequeña fracción de monoclínica. Las partículas de la muestra Z sintetizada mostraron formas irregulares y semihexagonales, aunque durante el tratamiento térmico cambiaron a formas esféricas o elipsoidales. Las partículas de la muestra ZK, tanto sintetizada como calcinada, presentaron formas prácticamente esféricas o elipsoidales. El tamaño medio de los cristales de las muestras sintetizadas Z y ZK fue 3.2 ± 0.8 y 5.5 ± 0.9 nm, respectivamente, mientras que el de las muestras calcinadas fue 8.5 ± 1.2 and 7.6 ± 1.2 nm, respectivamente.

Introduction

Zirconia (ZrO_2) based ceramics have being extensively investigated due to their excellent properties as either structural material (high toughness and strength, hardness, excellent chemical resistance, thermal shock resistance, high refractoriness, etc.), or as functional material (good ionic conductivity, relatively high electronic conductivity, low thermal conductivity at high temperature, biocompatibility, oxygen storage, etc.) [1–3]. All these properties make ZrO_2 ceramics to be excellent candidates for a wide number of applications, including catalysts, refractories, solid oxide fuel cells, thermal barriers, bioactive coatings, sensors, etc. [4–8]. The properties and performance of zirconia ceramics strongly depend on the physico-chemical properties of the starting powders, such as particle size distribution, specific surface area, crystalline structure, phase transformations, etc. Also, compared to conventional micrometer-sized zirconia, nanoscale zirconia materials have a wide functional diversity and exhibit enhanced or different properties, i.e., crystallite size plays an important role in property modification of materials. Therefore, the synthesis of zirconia nanocrystalline powders with controlled chemical composition, structure and monomodal distribution is essential to produce high performance nanophase and dense ceramics.

A literature survey revealed that zirconia nanoparticles have been synthesized by a broad variety of traditional methods, including solid state reaction [9], precipitation [10], hydrothermal [11], solvothermal [12], sol-gel [13], sol–gel-hydrothermal [14], freeze-drying [15], combustion [16], mechanochemical [17], non-hydrolytic thermal decomposition [18], sonochemical [19], thermal plasma [20], vapor phase hydrolysis [21], molten hydroxides [22], etc. Many of these methods require costly equipment, complex and tedious procedures, expensive precursors, multi-step reactions, precise pH control, organic templates, stabilizing or chelating agents, and thus are difficult to use and hard to control accurately. Typical drawbacks are inhomogeneity, varied particle size distribution, poor reactivity, low production rates, long reaction times, poor crystallinity particles that require an additional crystallization step at high temperatures, etc.

Conventional hydrothermal synthesis is one of the most successful methods for the preparation of monoclinic [23], tetragonal [24], cubic [25], and even orthorhombic (considered as an intermediate structure between monoclinic and tetragonal) [26] phases of submicrometer- and nanometer-sized crystalline zirconia powders. However, one of its major drawbacks is that, due to the slow heat transfer from the furnace to the steel vessel of the autoclave and to the reaction mixture inside, this technique generally involves very long reaction times, typically in the range of 12–24 h [23–25] and even up to 80 h [26], with temperatures about 200–250 °C.

The use of microwave irradiation as heating source for hydrothermal synthesis is a very promising route to produce inorganic nanostructured powders [27–30]. This is explained by the efficient microwave heating mechanism at molecular levels (i.e., internal and volumetric heating) which eliminates thermal gradients in the reaction system, providing a uniform environment for the reaction. The microwave-assisted hydrothermal process is considered the most effective technique for the synthesis of nano-powders due to the advantages over conventional hydrothermal technique, such as fast heating rate to reaction temperature, more uniform temperature distribution, enhanced crystallization kinetics, very short reaction times (typically, minutes to tens of minutes), formation of novel phases, great efficiency, high reproducibility and low production costs. These features allow the obtention of nanosized materials with high purity, controlled stoichiometry, good homogeneity, high crystallinity, uniform morphology and narrow particle size distribution. In addition, the microwave-assisted hydrothermal synthesis can be considered as environmentally friendly due to the reduction of energy and time consumption.

To the best of our knowledge, only a few reports on the microwave-assisted hydrothermal synthesis of pure zirconia [27,31–34] nanoparticles have been found in the available literature. Komarneni et al. [27] first reported a preliminary study on the microwave-hydrothermal synthesis of ZrO_2 from $ZrOCl_2{\cdot}8H_2O$, varying the precursor concentration (0.5 and 1 M), reaction temperature (164 and 194 °C) and reaction time (30 and 120 min), obtaining very poorly crystalline monoclinic zirconia, although the crystallinity increased with temperature and reaction time, as expected. Sathyaseelan et al. [31] prepared nanocrystalline ZrO_2 powder using $ZrOCl_2{\cdot}8H_2O$, 2-propanol and acetylene actone in the presence of a Triblock copolymer as structure directing agent, at 130 °C for 120 min, obtaining tetragonal single phase zirconia with an average particle size of 15 nm. Bondioli et al. [32] and Opalin-

ska et al. [33] synthesized well-crystallized ZrO_2 powders from $ZrOCl_2{\cdot}8H_2O$ and NaOH as precipitation agent, at 194 °C for 120 min and 270 °C for 20 min, respectively, obtaining nearly tetragonal single phase zirconia with a size range of powders very narrow (from 10 to 20 nm), in the first case, and monoclinic and tetragonal mixed phases with an average crystallite size of 11 nm, in the second one. Li et al. [34] prepared ZrO_2 powder using $ZrCl_4$ and NaOH, and studied the effects of reaction temperature (from 150 to 220 °C for 30 min) and solution pH values (2, 7 and 13) on the crystallization of ZrO_2, obtaining, depending on the conditions, amorphous $Zr(OH)_xO_y$, tetragonal single phase or a mixture of monoclinic and tetragonal phases of zirconia, with an average crystallite size in the range of 9–25 nm.

The aim of this work was to establish a simple, soft and rapid route for the synthesis of nanoparticles of zirconia, and their characterization, with high crystallinity and low particle size through a microwave-assisted hydrothermal method.

Experimental

Samples preparation

Microwave oven

A commercial Milestone ETHOS 1 (Sorisole, Italy) microwave oven specifically designed for synthetic applications operating at 2450 MHz and capable of programming and adjusting the most important reaction parameters (power, temperature, pressure and time) was used. A detailed description of the apparatus is shown in previous publications [35,36].

Chemicals

All chemical reagents in present work were of analytical grade and used as received without further purification. All aqueous solutions were prepared with deionized water with a resistivity of >18 MΩ cm, produced by a Milli-Q Plus pure water generating system from Millipore (Bedford, MA, USA). $ZrOCl_2{\cdot}8H_2O$ (Sigma–Aldrich, St. Louis, MO, USA) and KOH (Panreac, Barcelona, Spain) were used as starting materials.

Stock solution ≈1 M of $ZrOCl_2{\cdot}8H_2O$ was prepared, and it was standardized by Inductively Coupled Plasma Optical Emission Spectrometry (ICP-OES) by using a Thermo Jarrell Ash spectrometer, Model Iris Advantage Duo (Waltham, MA, USA). For the standardization of the stock solution, as well as for the determination of Zr in the supernatant liquid, the calibration was performed with standard solutions of appropriate concentration prepared by serial aqueous dilution from standard stock solutions of $1.000 \pm 0.002\ g\,l^{-1}$ of Zr (Merck, Darmstadt, Germany). As analytical line, the wavelength at 339.197 nm of Zr was used.

Procedure

All the reactions were carried out in a 100 ml sealed vessel made of high-purity TFM, which is surrounded by a safety shield. Temperature and pressure during synthesis were monitored and controlled with the aid of a shielded thermocouple inserted directly into the vessel and with a pressure transducer sensor connected to the vessel. Built-in magnetic stirring (Teflon-coated stirring bar) was used. The evolution of time, temperature, pressure and power were continuously recorded during each experiment.

Synthesis of zirconia by decomposition of $ZrOCl_2{\cdot}8H_2O$. 25 mmol of $ZrOCl_2{\cdot}8H_2O$ (from standardized stock solution) and 25 ml of H_2O were put into the 100 ml vessel of the microwave oven, keeping a constant stirring. The vessel was sealed and placed in the microwave oven, where it was heated to a temperature of 180 °C at a rate of $0.25\ °C\,s^{-1}$ and held at this temperature for 20 min. This sample was labeled as Z.

Synthesis of zirconia by precipitation of $ZrOCl_2{\cdot}8H_2O$ with KOH and dehydration of hydroxides. 25 mmol of $ZrOCl_2{\cdot}8H_2O$ (from standardized stock solution) and 19 ml of H_2O were put into the 100 ml vessel of the microwave oven, keeping a constant stirring. Under continuous stirring, 4.90 ml of 10 N KOH were added dropwise, and then 1 N KOH (about 1 ml), also dropwise, until a pH of 10 ± 0.2 was reached. Immediate formation of a white large colloidal solid was observed. The vessel was sealed and placed in the microwave oven, where it was heated to a temperature of 180 °C at a rate of $0.25\ °C\,s^{-1}$ and held at this temperature for 20 min. This sample was labeled as ZK.

In all cases, after cooling down at room temperature, a white suspension was obtained. The separation of the solid from the liquid was performed by centrifugation using a multipurpose bench top centrifuge at a gyration speed of 2400 rpm (Núve NF800, Ankara, Turkey). The obtained particles, of white color, were collected, carefully washed several times with deionized water until chloride ions were no longer detectable in the washing water ($AgNO_3$ test) and centrifuged every time, and finally dried overnight in air at 110 °C. The dried material was crushed using an agate mortar and sieved through a 100 μm sieve. A portion of the powders was calcined at 500 °C for 1 h in air at a heating rate of $10\ °C\,min^{-1}$.

Characterization techniques

The crystalline phases of the as-synthesized and calcined powders were determined by X-ray diffraction (XRD) on a D8 Advance (Bruker, Karlsruhe, Germany) diffractometer using Cu K_α radiation. The measurements were performed within 2θ angles ranging from 20° to 80° at 25 °C, and the step size and time of reading were 0.02° and 2 s, respectively. The following XRD patterns collected at the ICDD© databank (Joint Committee for Powder Diffraction Standards, JCPDS-The International Centre for Diffraction Data©, Newtown Square, PA, USA) were used as references for the analysis of our XRD patterns: PDF card 00-037-1484 of monoclinic zirconia and PDF card 00-048-0224 of tetragonal zirconia.

The morphology, size and microstructure of the powders was studied by electron microscopy: field emission scanning electron microscopy (FE-SEM) on a S-4800 Type I (Hitachi, Tokyo, Japan) microscope; and high-resolution transmission electron microscopy (HR-TEM) on a JEM-2100F (JEOL, Tokyo, Japan) microscope working at 200 keV, complemented by selected area electron diffraction (SAED). The image processing was performed using the DigitalMicrograph® software. The particle size distribution, mean size diameter (D_0) and standard deviation (σ) were determined using the ImageJ soft-

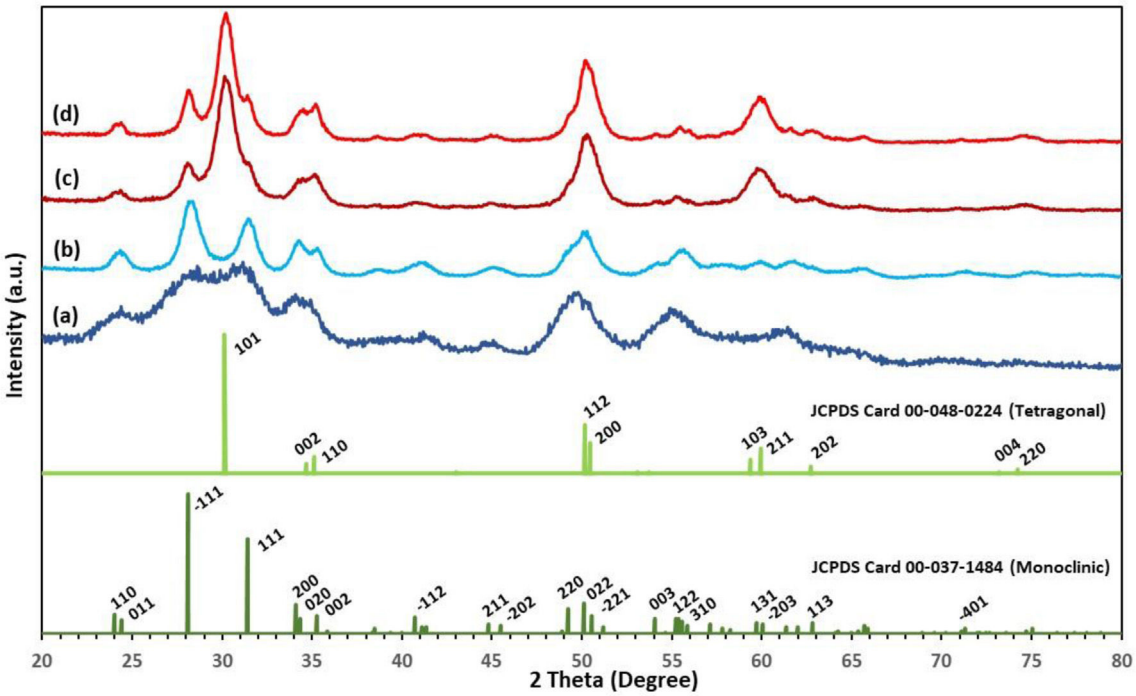

Fig. 1 – XRD patterns of samples Z (a, b) and ZK (c, d) as-synthesized (a, c) and calcined at 500 °C (b, d). JCPDS Card 00-037-1484 of monoclinic zirconia and JCPDS Card 00-048-0224 of tetragonal zirconia are also included.

ware after measuring at least 100 particles in random fields of view on the HR-TEM micrographs.

Results and discussion

Powder synthesis

The synthesis of pure zirconia has been done in two ways. In the first way, the decomposition of $ZrOCl_2{\cdot}8H_2O$ under the effect of temperature by the microwave radiation leads to the direct formation of a ZrO_2 precipitate (sample Z), according to the Eq. (1).

$$ZrOCl_2 \cdot 8H_2O \overset{MW\,\Delta}{\rightarrow} ZrO_2 \downarrow + 2HCl + 7H_2O. \quad (1)$$

In the second one, the general chemical reaction takes place in two steps. In the first step, the precipitation of zirconium hydroxide under strong alkaline pH conditions by addition of KOH occurs according to Eq. (2). In the second step, the dehydration of hydroxide by microwave heating leads to the formation of the zirconia (sample ZK), according to Eq. (3). The overall chemical reaction is shown in Eq. (4).

$$ZrOCl_2 \cdot 8H_2O + 2KOH \rightarrow Zr(OH)_4 \downarrow + 2KCl + 7H_2O. \quad (2)$$

$$Zr(OH)_4 \downarrow \overset{MW\,\Delta}{\rightarrow} ZrO_2 \downarrow + 2H_2O. \quad (3)$$

$$ZrOCl_2 \cdot 8H_2O + 2KOH \overset{MW\,\Delta}{\rightarrow} ZrO_2 \downarrow + 2KCl + 9H_2O. \quad (4)$$

$ZrOCl_2{\cdot}8H_2O$ is a very hygroscopic compound. Consequently, it cannot be dried to eliminate moisture, so it is very difficult to quantitatively weigh an accurate quantity of the product. Because of this, stock solution of $ZrOCl_2{\cdot}8H_2O$ was prepared with a concentration approximately 1 M, and it was standardized by ICP-OES, which ensures the use of stoichiometric amount of Zr. Thus, considering that the volume range in the vessel is 8-50 ml, 25 ml of $ZrOCl_2{\cdot}8H_2O$ stock solution are added to the vessel for all syntheses, in addition to 25 ml of H_2O for synthesis of sample Z and 6 ml of KOH and 19 ml of H_2O for synthesis of sample ZK. Under these conditions,the volume of all reagents in all syntheses was practically thesame (about 50 ml).

It is very important to perform a complete washing of the particles obtained directly from the microwave reactor in order to fully eliminate the KCl. The presence of this compound causes two problems: first, it presents a strong diffraction peak at $2\theta \approx 28^\circ$ (PDF Card 00-041-1476 of sylvite, KCl), which overlaps with the reflection (−111) at $2\theta = 28.2^\circ$ of the monoclinic phase of zirconia; and second, it contaminates the synthesized zirconia powders. In this regard, silver nitrate is a common and simple test for chloride ions in aqueous solutions and is extremely sensitive.

The global time of the microwave-assisted hydrothermal synthetic procedure is lower than 1 h (10 min for heating from room temperature to 180 °C, 20 min of dwell time and about 20–30 min for cooling to room temperature). The pressure reached during heating was around 9 bar.

Analytical control of the microwave synthesis

In order to study the degree of precipitation of the Zr involved in the microwave synthesis, the content of this element in

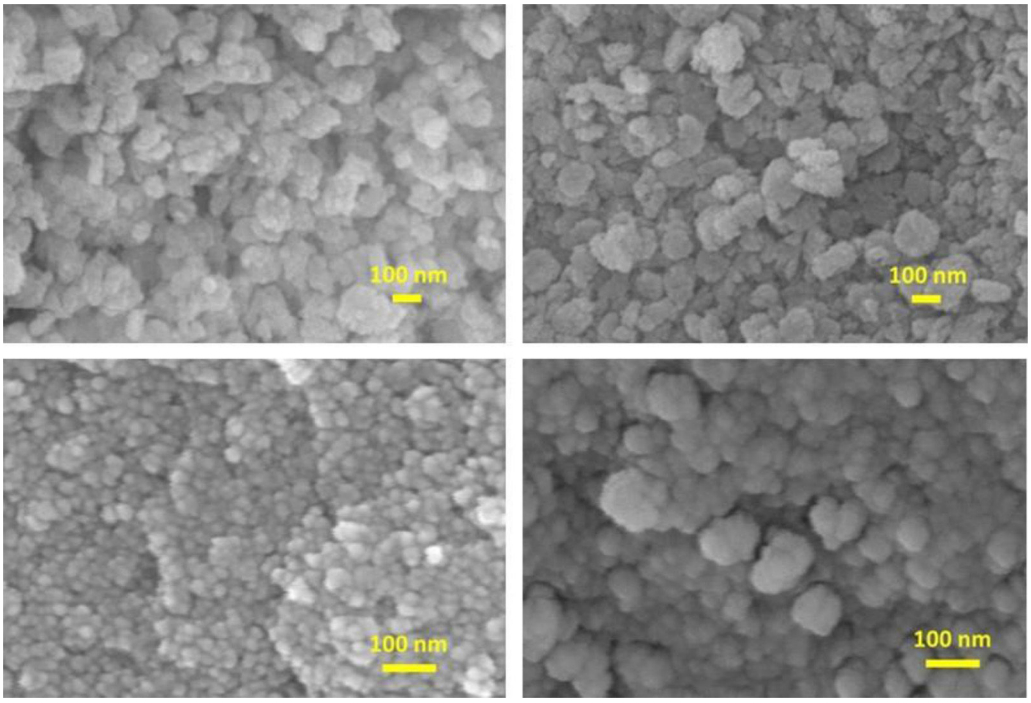

Fig. 2 – FE-SEM images of samples Z (top) and ZK (bottom) as-synthesized (left side) and calcined at 500 °C (right side).

the supernatant liquid after the completion of microwave-assisted synthesis was determined by ICP-OES. The analytical results for the two syntheses (i.e., for samples Z and ZK) showed that the concentration of Zr in both cases was below its quantification limit (about 0.007 mg Zr l^{-1} for our ICP-OES equipment). This means that the content of Zr in the supernatant liquids was lower than 0.0007 mg, corresponding to 0.000008 mmol $ZrOCl_2{\cdot}8H_2O$, which verified the quantitative precipitation (higher than 99.9999%) of this element in the two synthetic routes.

Phase development

The crystalline phases of the powders were determined by XRD. The XRD patterns of the Z and ZK powder particles, both in their as-synthesized condition and after the calcination at 500 °C for 1 h in air, are depicted in Fig. 1.

Fig. 1a shows the XRD pattern of the zirconia obtained by decomposition of $ZrOCl_2{\cdot}8H_2O$ (sample Z) just as-synthesized. As it can be observed, it shows a crystalline behavior with well-defined reflections. All reflections can be clearly indexed to the monoclinic phase of zirconia. The thermal treatment provides enhanced crystallinity, as it can be seen in Fig. 1b. From the spectra, it can be concluded that there is only one single crystalline phase, the monoclinic phase, in sample Z after the synthesis and after the thermal treatment. This result agrees with that obtained by Komarneni et al. [27], who also performed a synthesis of ZrO_2 by direct decomposition of $ZrOCl_2{\cdot}8H_2O$.

Similarly, zirconia powders obtained from $ZrOCl_2{\cdot}8H_2O$ after precipitation with KOH and dehydration of hydroxides (sample ZK) were also characterized before and after the above-mentioned thermal treatment. The crystalline phases obtained just after the synthesis and after the thermal treatment can be observed in Fig. 1c and d, respectively. From the observation of these spectra, the following conclusions can be drawn: (1) the precipitation of hydroxide before the oxide formation has a clear effect in the development of the crystalline phases, leading to a powder with tetragonal as the major phase, although a minor fraction of monoclinic is also present; (2) the powders synthesized with KOH seem to be more crystalline than those obtained without precipitation with the base; (3) the thermal treatment at 500 °C do not have a significant effect on either the crystallinity or the phases relative ratio, which are maintained nearly constant in the temperature range considered. The occurrence of metastable tetragonal phase is attributed to the effect of the critical crystallite size, as reported by Garvie [37], who experimentally showed the existence of a critical size of about 30 nm, below which the tetragonal phase is stable. That is, the tetragonal phase can be obtained directly during microwave synthesis of nanocrystalline powders. Other publications on microwave-assisted hydrothermal synthesis of ZrO_2 report obtaining powders with monoclinic and tetragonal mixed phases [33,34], as in the present work, or with tetragonal single phase [31,32,34], depending on the synthesis conditions.

From all XRD patterns displayed in Fig. 1, no peaks of other impurity phases are observed, indicating a high purity of the obtained samples. On the other hand, the significant broadening of the peaks can be attributed to the nanocrystalline nature of the prepared powders, as will be shown below.

Microstructure and morphology

The surface morphology and approximate particle size were evaluated for all samples by FE-SEM observations. Fig. 2 shows the FE-SEM images of the synthesized powders as obtained and after calcining at 500 °C for 1 h. In all cases, the images

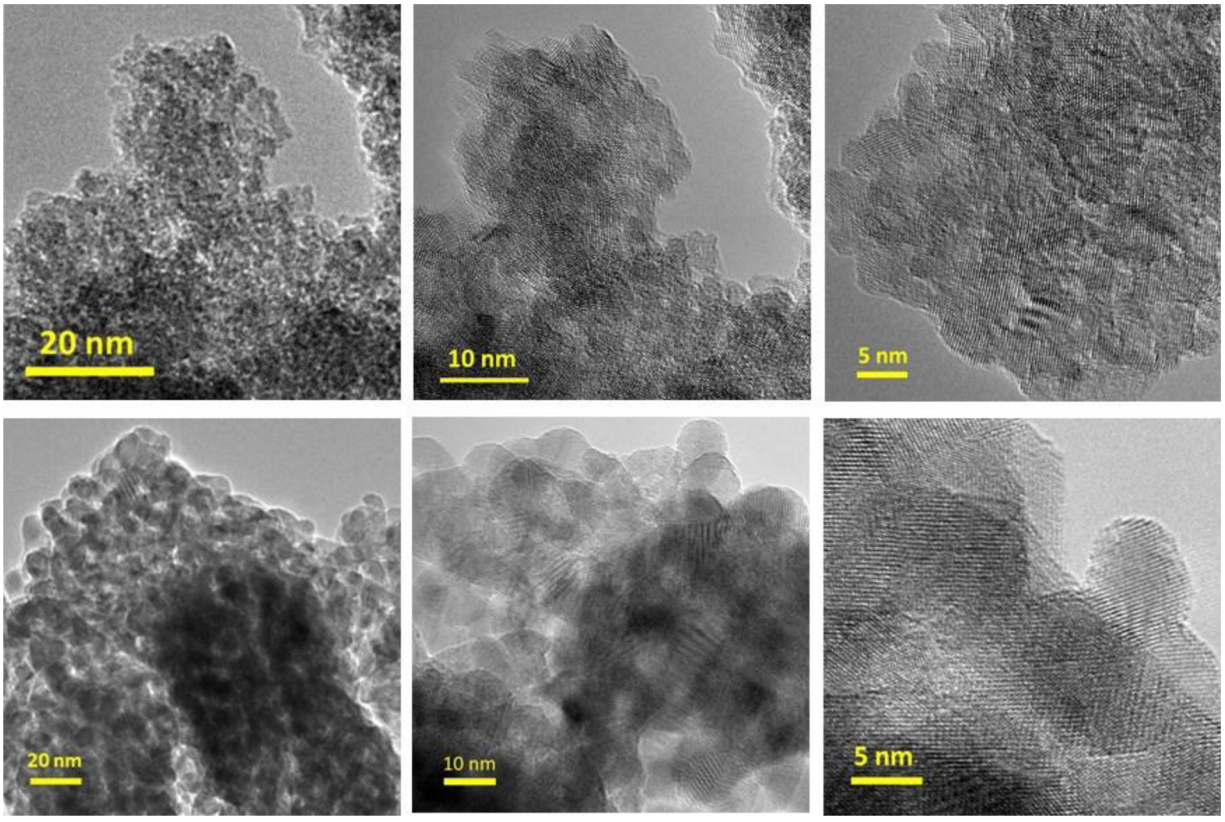

Fig. 3 – HR-TEM images at different magnifications of sample Z as-synthesized (top) and calcined at 500 °C (bottom).

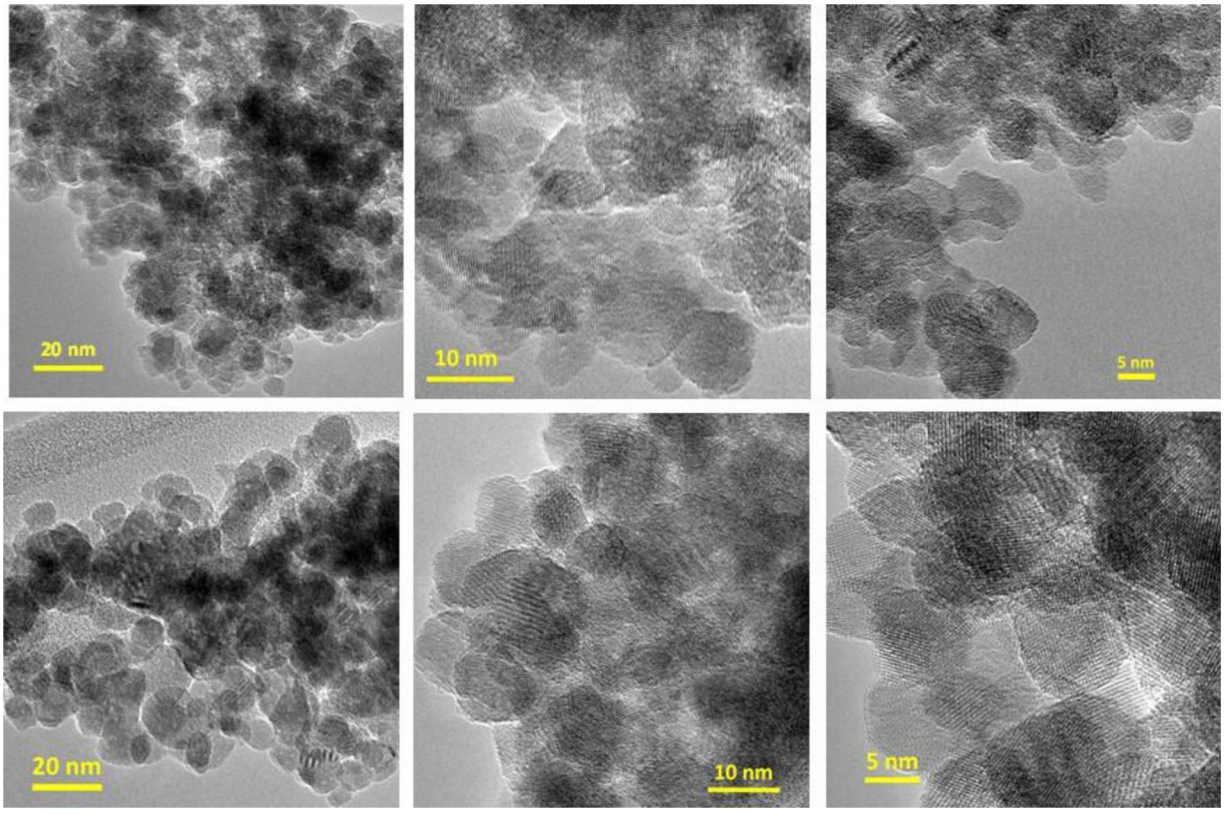

Fig. 4 – HR-TEM images at different magnifications of sample ZK as-synthesized (top) and calcined at 500 °C (bottom).

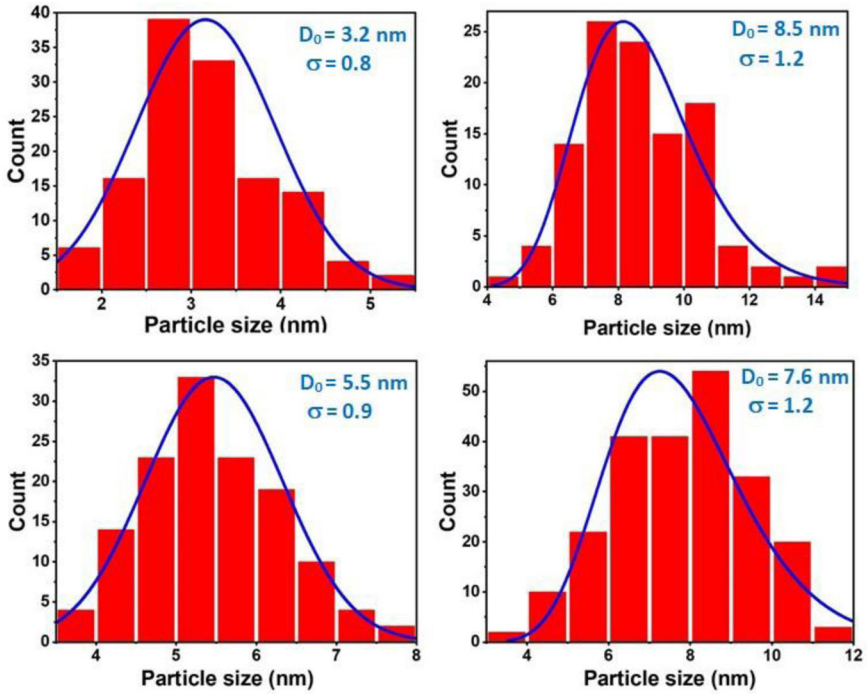

Fig. 5 – Particle size distribution of samples Z (top) and ZK (bottom) as-synthesized (left side), fitted with a normal function (solid line), and calcined at 500 °C (right side), fitted with a log-normal function (solid line). Mean size diameter (D_0) and standard deviation (σ) values are included.

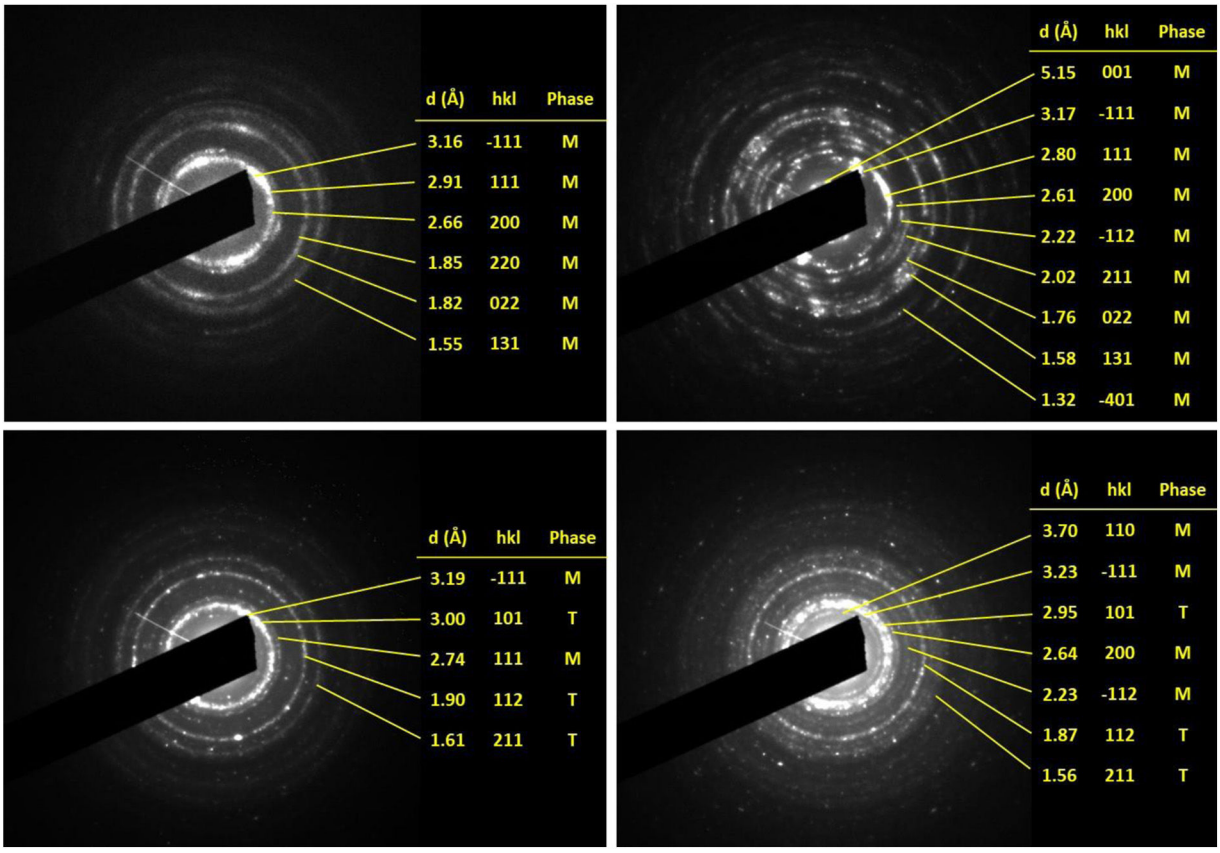

Fig. 6 – SAED patterns of samples Z (top) and ZK (bottom) as-synthesized (left side) and calcined at 500 °C (right side), including the interplanar distance (d), the Miller indices (h, k, l) and the crystalline phases monoclinic (M) and tetragonal (T).

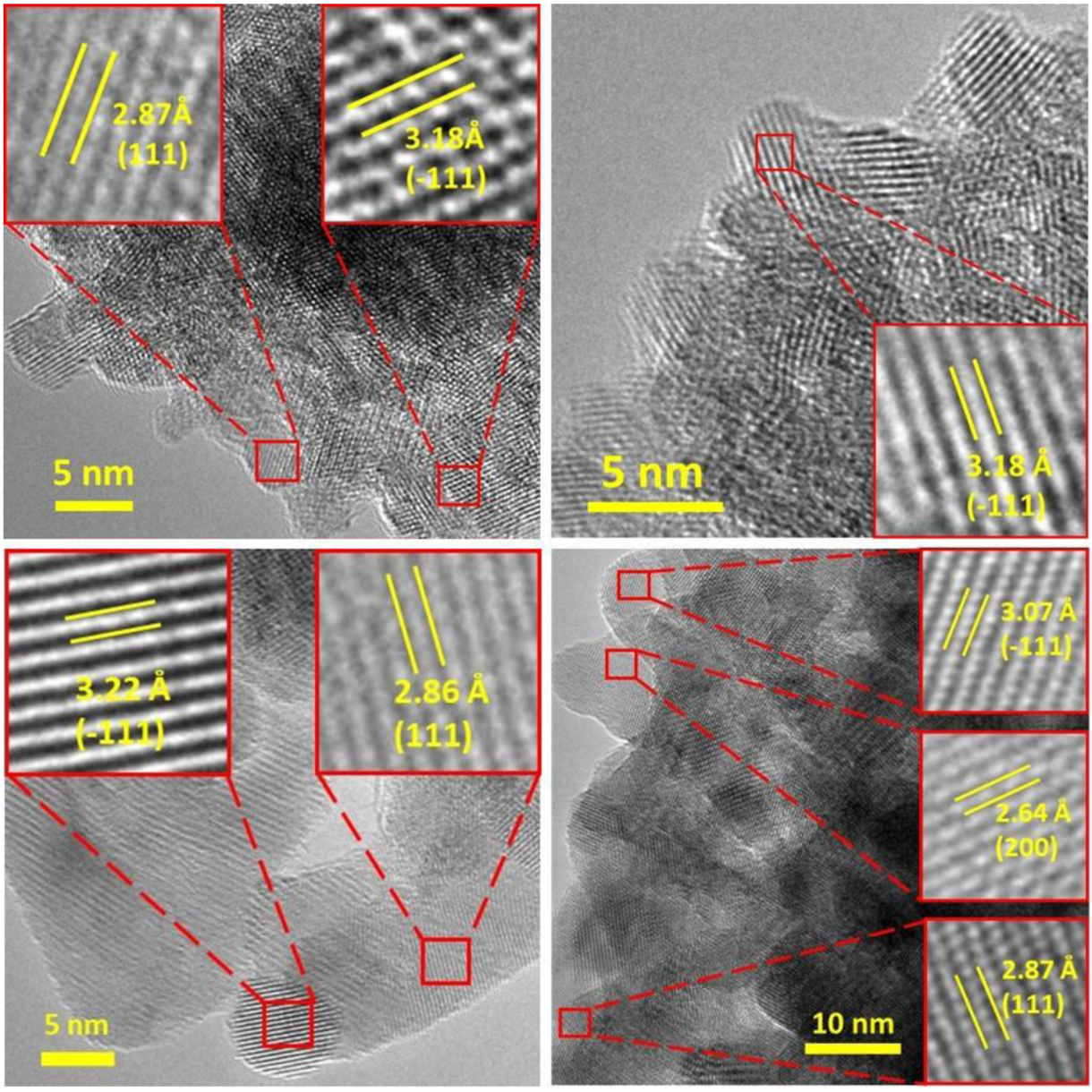

Fig. 7 – HR-TEM images at higher magnifications showing lattice fringe patterns (insets) of individual nanocrystals of sample Z as-synthesized (top) and calcined at 500 °C (bottom).

reveal that particles are in the nanometer range and apparently spherical in shape, although they are agglomerated, due to the inter-particle forces effect, forming clusters of 50–150 nm and <25 nm for as-synthesized samples Z and ZK, respectively. After the thermal treatment at 500 °C, the particle size of the sample Z does not increase very much, maintaining an average size of about 100 nm. The sample ZK has increased particle size after heating at 500 °C, but it remains always lower than the average size of the Z one. This seems to indicate that the powder obtained by precipitation and dehydration of the hydroxide helps to a more effective dispersion of the particles, which agglomerate to a lower extent than in the case of the direct formation of the oxide by decomposition of $ZrOCl_2 \cdot 8H_2O$.

HR-TEM and SAED studies were carried out in order to obtain structural information (i.e., morphology, crystallinity, crystal size and nanostructure) about the prepared powders.

Figs. 3 and 4 show representative HR-TEM images at different magnifications of the as-synthesized and calcined samples Z and ZK, respectively. From these images, it is clear that, in all cases, the particles are polycrystalline, consisting of smaller single crystallites with a typical diameter lower than 10 nm. However, there are some differences in the shape of the particles. The particles of the as-synthesized sample Z have irregular and semi-hexagonal shapes, although they change to spherical or ellipsoidal shapes during heat treatment. The particles of the sample ZK, both as-synthesized and calcined, exhibit nearly spherical or ellipsoidal shapes.

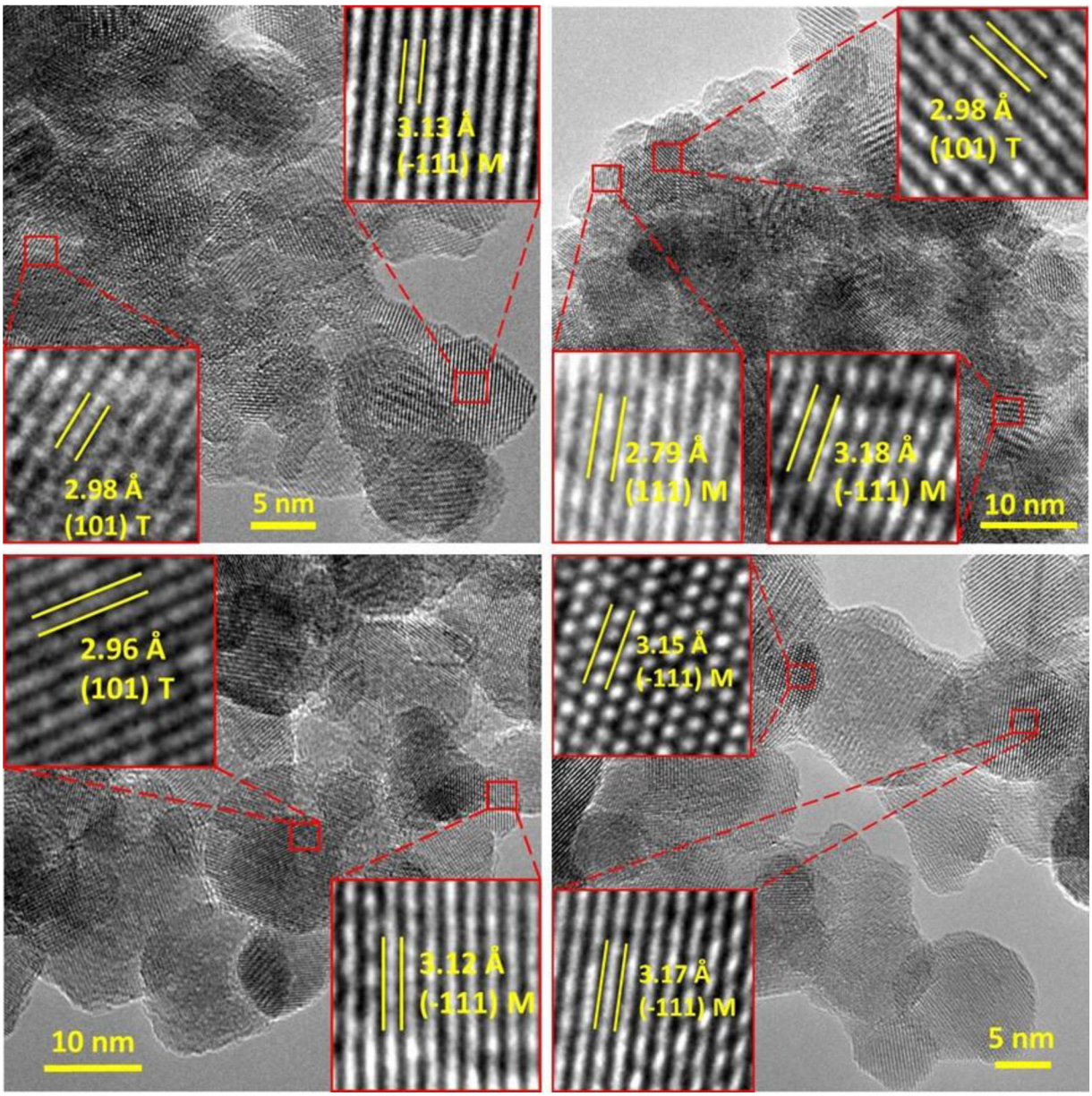

Fig. 8 – HR-TEM images at higher magnifications showing lattice fringe patterns (insets) of individual nanocrystals of sample ZK as-synthesized (top) and calcined at 500 °C (bottom).

Fig. 5 illustrates the particle size distribution of the as-synthesized and calcined samples Z and ZK. It includes the D_0 and σ values, which have been accurately calculated by fitting the particle size distribution histogram to the normal distribution function, in the case of as-synthesized samples, and to the log-normal distribution function, in the case of calcined samples. As it can be seen, D_0 values for as-synthesized samples Z and ZK are 3.2 and 5.5 nm along with σ values of 0.8 and 0.9 nm, respectively. As expected, the thermal treatment of the samples increases the D_0 values, considerably for sample Z and slightly for sample ZK: 8.5 and 7.6 nm, respectively, with the same σ value of 1.2 nm.

Fig. 6 depicts the SAED patterns of as-synthesized and calcined samples Z and ZK. It also includes the interplanar distances (the *d*-spacing, i.e., the distance between crystal planes), which have been calculated from the diameter measurement of each ring, the corresponding Miller indices (hkl), and the monoclinic (M) and tetragonal (T) crystalline phases. For all samples, the SAED pattern exhibits a series of clear concentric diffraction rings with intermittent spots, indicating the polycrystalline nature of the nanosized zirconia powders. As it can be seen, the SAED pattern of the as-synthesized sample Z confirms the existence of monoclinic mono-phase of ZrO_2. In the SAED pattern of the as-synthesized sample ZK, all the rings can be clearly indexed to the monoclinic and tetragonal crystal systems. On the other hand, the SAED patterns of the two calcined zirconia samples are similar to those of the corresponding as-synthesized samples, but they exhibit more and brighter rings, which is due to their higher crystallinity. Regarding crystallinity and composition of the

crystalline phases, all SAED results are consistent with the XRD results presented above.

Figs. 7 and 8 illustrate HR-TEM images at higher magnifications of the as-synthesized and calcined samples Z and ZK, respectively. They also include the measured distance between every two successive fringes (i.e., the *d*-spacing), the corresponding hkl indices and the M and T crystalline phases. The insets show well-ordered equidistant parallel lattice fringe patterns of individual nanocrystals, which confirms the high crystallinity of the two samples, even of the as-synthesized ones. In Fig. 7, crystallites with measured *d*-spacing of 3.07–3.22 Å, 2.86–2.87 Å and 2.64 Å are observed, which is consistent with the Miller indices of the most characteristics planes (−111), (111) and (200), respectively, of monoclinic zirconia. In Fig. 8, crystallites are seen with measured *d*-spacing corresponding to the (−111) and (111) planes of monoclinic zirconia, as well as with measured *d*-spacing of 2.96–2.98 Å which can be attributed to the well-recognized lattice *d*-spacing of the (101) plane of tetragonal zirconia. These results agree with those obtained by XRD and SAED reported previously.

Conclusions

It has been demonstrated that the microwave-assisted hydrothermal synthesis provides a simple, soft, fast, and energy efficient route for the preparation of nanosized zirconia powders. Two synthesis routes have been proposed, one by direct decomposition of $ZrOCl_2{\cdot}8H_2O$ and another by precipitation of $ZrOCl_2{\cdot}8H_2O$ with KOH and dehydration of hydroxides, which lead to the formation of pure monoclinic zirconia, in the first case, and tetragonal zirconia (with a small fraction of monoclinic), in the second one. In both cases, the synthetic procedure is very gentle and rapid (10 min heating from room temperature to 180 °C and 20 min dwell time) and is carried out in an aqueous medium, without the need for organic solvents, templates, stabilizing or chelating agents, etc., so it can be considered as environmentally friendly. The as-synthesized nanoparticles obtained by the two proposed synthesis routes present a high degree of crystallinity and an average diameter lower than 10 nm.

Conflict of interest

The author declares that he has no known competing financial interests or personal relationships that could have appeared to influence the work reported in this paper.

Acknowledgements

This research has been carried out with financial support from the Spanish Ministry of Science, Innovation and Universities (MCIU), the State Research Agency (AEI) and the European Regional Development Fund (FEDER) through the Project PID2021-124521OB-I00.

REFERENCES

[1] R. Stevens, An Introduction to Zirconia, Magnesium Elektron Ltd, Twickenham, UK, 1986.
[2] O.A. Graeve, Zirconia (Chapter 10), in: J.F. Shackelford, R.H. Doremus (Eds.), Ceramic and Glass Materials: Structure, Properties and Processing, Springer, Boston, MA, USA, 2008, pp. 169–197.
[3] A.H. Heuer, L.W. Hobbs, Science and Technology of Zirconia. Advances in Ceramics, vol. 12, The American Ceramic Society, Columbus, OH, USA, 1981.
[4] R.C. Garvie, R.H. Hannink, R.T. Pascoe, Ceramic steel? Nature 258 (1975) 703–704.
[5] J. Chevalier, What future for zirconia as a biomaterial? Biomaterials 27 (2006) 535–543.
[6] A. Atkinson, S. Barnett, R.J. Gorte, J.T.S. Irvine, A.J. McEvoy, M. Mogensen, S.C. Singhal, J. Vohs, Advanced anodes for high-temperature fuel cells, Nature Mater. 3 (2004) 17–27.
[7] W.C. Maskell, Progress in the development of zirconia gas sensors, Solid State Ionics 134 (2000) 43–50.
[8] K. Tanabe, T. Yamaguchi, Acid–base bifunctional catalysis by ZrO_2 and its mixed oxides, Catal. Today 20 (1994) 185–198.
[9] V.V. Mishra, A.K. Garg, D.C. Agrawal, Preparation of tetragonal zirconia powders by a solid state reaction: kinetics, phases and morphology, Bull. Mater. Sci. 21 (1998) 81–86.
[10] S.K. Tadokoro, E.N.S. Muccillo, Synthesis and characterization of nanosized powders of yttria-doped zirconia, J. Alloys Comp. 344 (2002) 186–189.
[11] S. Somiya, T. Akiba, Hydrothermal zirconia powders: a bibliography, J. Eur. Ceram. Soc. 19 (1999) 81–87.
[12] L. Liu, S. Wang, G. Jiang, B. Zhang, J. Yang, J. Wang, W. Liu, Y. Li, H. Liu, Solvothermal synthesis of zirconia nanomaterials: latest developments and future, Ceram. Int. 48 (2022) 32649–32676.
[13] C. Viazzi, A. Deboni, J.Z. Ferreira, J.P. Bonino, F. Ansart, Synthesis of yttria stabilized zirconia by sol–gel route: influence of experimental parameters and large scale production, Solid State Sci. 8 (2006) 1023–1028.
[14] Q. Chang, J. Zhou, Y. Wang, G. Meng, Formation mechanism of zirconia nano-particles containing pores prepared via sol–gel-hydrothermal method, Adv. Powder Technol. 21 (2010) 425–430.
[15] C. Tallón, R. Moreno, M.I. Nieto, Synthesis of ZrO_2 nanoparticles by freeze drying, Int. J. Appl. Ceram. Technol. 6 (2009) 324–334.
[16] K.R. Venkatachari, D. Huang, S.P. Ostrander, W.A. Schulze, G.C. Stangle, A combustion synthesis process for synthesizing nanocrystalline zirconia powders, J. Mater. Res. 10 (1995) 748–755.
[17] T.D. Isfahani, J. Javadpour, A. Khavandi, R. Dinnebier, H.R. Rezaie, M. Goodarzi, Mechanochemical synthesis of zirconia nanoparticles: formation mechanism and phase transformation, Int. J. Refract. Metals Hard Mater. 31 (2012) 21–27.
[18] R. Malakooti, H. Mahmoudi, R. Hosseinabadi, S. Petrov, A. Migliori, Facile synthesis of pure non-monoclinic zirconia nanoparticles and their catalytic activity investigations for Knoevenagel condensation, RSC Adv. 3 (2013) 22353–22359.
[19] S. Zinatloo-Ajabshir, M. Salavati-Niasari, Synthesis of pure nanocrystalline ZrO_2 via a simple sonochemical-assisted route, J. Ind. Eng. Chem. 20 (2014) 3313–3319.
[20] A.B. Nawale, N.S. Kanhe, S.V. Bhoraskar, V.L. Mathe, A.K. Das, Influence of crystalline phase and defects in the ZrO_2

nanoparticles synthesized by thermal plasma route on its photocatalytic properties, Mater. Res. Bull. 47 (2012) 3432–3439.
[21] G. Shi, F. Yu, Y. Wang, R. Li, Synthesis of growth-controlled ZrO_2 nanocrystals via vapor phase hydrolysis, Ceram. Int. 40 (2014) 13083–13088.
[22] L. Wang, K.F. Cai, Y.Y. Wang, J.L. Yin, H. Li, C.W. Zhou, Preparation and characterization of tetragonal-ZrO_2 nanopowders by a molten hydroxides method, Ceram. Int. 35 (2009) 2499–2501.
[23] L. Kumari, W.Z. Li, J.M. Xu, R.M. Leblanc, D.Z. Wang, Y. Li, H. Guo, J. Zhang, Cryst. Growth Des. 9 (2009) 3874–3880.
[24] C.V. Reddy, B. Babu, I.N. Reddy, J. Shim, Synthesis and characterization of pure tetragonal ZrO_2 nanoparticles with enhanced photocatalytic activity, Ceram. Int. 44 (2018) 6940–6948.
[25] M.N. Tahir, L. Gorgishvili, J. Li, T. Gorelik, U. Kolb, L. Nasdala, W. Tremel, Facile synthesis and characterization of monocrystalline cubic ZrO_2 nanoparticles, Solid State Sci. 9 (2007) 1105–1109.
[26] C.R. Babu, N.R.M. Reddy, K. Reddy, Synthesis and characterization of high dielectric nano zirconium oxide, Ceram. Int. 41 (2015) 10675–10679.
[27] S. Komarneni, R. Roy, Q.H. Li, Microwave-hydrothermal synthesis of ceramic powders, Mater. Res. Bull. 27 (1992) 1393–1405.
[28] I. Bilecka, M. Niederberger, Microwave chemistry for inorganic nanomaterials synthesis, Nanoscale 2 (2010) 1358–1374.
[29] M. Baghbanzadeh, L. Carbone, P.D. Cozzoli, C.O. Kappe, Microwave-assisted synthesis of colloidal inorganic nanocrystals, Angew. Chem. Int. Ed. 50 (2011) 11312–11359.
[30] Y.-J. Zhu, F. Chen, Microwave-assisted preparation of inorganic nanostructures in liquid phase, Chem. Rev. 114 (2014) 6462–6555.
[31] B. Sathyaseelan, E. Manikandan, I. Baskaran, K. Senthilnathan, K. Sivakumar, M.K. Moodley, R. Ladchumananandasivam, M. Maaza, Studies on structural and optical properties of ZrO_2 nanopowder for opto-electronic applications, J. Alloys Compd. 694 (2017) 556–559.
[32] F. Bondioli, A.M. Ferrari, C. Leonelli, C. Siligardi, G.C. Pellacani, Microwave-hydrothermal synthesis of nanocrystalline zirconia powders, J. Am. Ceram. Soc. 84 (2001) 2728–2730.
[33] A. Opalinska, I. Malka, W. Dzwolak, T. Chudoba, A. Presz, W. Lojkowski, Size-dependent density of zirconia nanoparticles, Beilstein J. Nanotechnol. 6 (2015) 27–35.
[34] C. Li, K. Li, H. Li, Y. Zhang, H. Ouyang, L. Liu, C. Sun, Effect of reaction temperature on crystallization of nanocrystalline zirconia synthesized by microwave-hydrothermal process, J. Alloys Compd. 561 (2013) 23–27.
[35] M.T. Colomer, I. Delgado, A.L. Ortiz, J.C. Fariñas, Microwave-assisted hydrothermal synthesis of single-crystal nanorods of rhabdophane-type Sr-doped $LaPO_4$ nH_2O, J. Am. Ceram. Soc. 97 (2014) 750–758.
[36] J.C. Fariñas, R. Moreno, A. Pérez, M.A. García, M. García-Hernández, M.D. Salvador, A. Borrell, Microwave-assisted solution synthesis, microwave sintering and magnetic properties of cobalt ferrite, J. Eur. Ceram. Soc. 38 (2018) 2360–2368.
[37] R.C. Garvie, The occurrence of metastable tetragonal zirconia as a crystallite size effect, J. Phys. Chem. 69 (1965) 1238–1243.